Title
A simulation study on condensation risk in radiant cooling panels with elevated air movement

Journal
2026 IAQVEC Conference

Authors
Park, Jiwon
Lee, Sangjoon
Li, Jiayu
et al.

Publication Date
2026

A simulation study on condensation risk in radiant cooling panels with elevated air movement

Jiwon Park[1,2*], *Sangjoon* Lee[3,4], *Jiayu* Li[1], *Kian Wee* Chen[5,6], *Ippei* Izuhara[5,6,7], and *Stefano* Schiavon[1,2,8]

[1]Center for the Built Environment, University of California, Berkeley, USA
[2]Department of Architecture, University of California, Berkeley, USA
[3]Department of Aeronautics and Astronautics, Stanford University, USA
[4]School of Mechanical and Aerospace Engineering, Nanyang Technological University, Singapore
[5]Andlinger Center for Energy and the Environment, Princeton University, USA
[6]Global Environmental Technologies Inc., USA
[7]Sanken Setsubi Kogyo CO., LTD., Japan
[8]Department of Civil and Environmental Engineering, University of California, Berkeley, USA

Abstract. Radiant cooling panels are an energy-efficient heating, ventilation, and air conditioning (HVAC) alternative to conventional all-air systems, as they operate with higher chilled water temperatures and rely on water as the primary heat transfer medium. However, their wider adoption has been constrained by the risk of surface condensation, which limits allowable surface temperatures and reduces cooling capacity. Elevated air movement, such as that induced by ceiling fans, has been proposed as a strategy to enhance cooling capacity and maintain thermal comfort, yet its impact on condensation behavior remains insufficiently understood, particularly under conditions where panel surfaces operate below the dew point. This study employs transient computational fluid dynamics (CFD) simulations using the interThermalPhaseChangeFoam solver in OpenFOAM to investigate the effects of air speed on condensation phenomena over a uniformly cooled radiant panel. A simplified numerical wind tunnel containing a small-scale radiant panel element is simulated to isolate airflow effects on phase change behavior with air temperatures of 22-27 °C, relative humidity levels of 50-60%, air velocities ranging from 0-3 m/s, and panel surface temperatures set 0.5-2.0 °C below the dew point. The analysis focuses on steady-state phase change heat flux and equivalent water thickness on the panel surface. Results show that increasing subcooling temperature (defined as the difference between the panel surface temperature and the dew-point temperature of the surrounding air) consistently increases both phase change heat and equivalent water thickness. In contrast, the influence of air speed on phase change heat is strongly dependent on subcooling level, exhibiting non-monotonic behavior at higher subcooling conditions. Meanwhile, the equivalent water thickness decreases monotonically with increasing air velocity across all cases, indicating enhanced removal of condensed water by airflow. These findings demonstrate that condensation risk cannot be assessed using a single metric alone and highlight the importance of jointly considering latent heat transfer and surface water retention. The results further suggest that, under appropriate subcooling and airflow conditions, elevated air movement may enable increased cooling capacity while mitigating practical condensation risks in radiant cooling applications.

Keywords. Radiant cooling, Condensation risk, Computational fluid dynamics

1 Introduction

Ceiling fans can improve radiant systems' cooling and heating capacity by increasing air movement. In cooling applications, fans enable higher cooling setpoints without compromising thermal comfort, thus reducing energy use. For example, Karmann et al. (2018) investigated fan-assisted radiant systems, finding that cooling capacity increased by 12–26% with different fan configurations. In addition, fans extended the comfort operative temperature range by up to 2.9 °C, from 26.0 °C to 28.9 °C [1].

While the benefits of fan-assisted airflow for thermal comfort and energy savings are well established, the impact of elevated air speeds on condensation behavior at radiant cooling panels remains underexplored. This issue is particularly relevant in scenarios where warm and humid air may be introduced into indoor spaces through infiltration or unintended ventilation [2]. Previous studies

* Corresponding author: jiwonpark@berkeley.edu

indicate that air speed influences surface mass transfer, but whether evaporation or condensation occurs depends on the thermodynamic conditions at the surface, particularly the surface temperature relative to the dew point. Zhang et al. (2022) showed that under dry conditions, higher air speeds supplied to a cooled surface reduced evaporation time [3]. In contrast, Salins et al. (2021) reported that for a cooled coil operating below the dew point, condensation increased with air velocity only up to a critical value (1.95 m/s), beyond which the accumulated condensate decreased despite continued high airflow [4]. These observations indicate that the relationship between air speed and condensation is not monotonic, even for surfaces operating below the dew point, and that the conditions governing the transition between condensation enhancement and suppression remain unclear.

Therefore, CFD simulations are employed to investigate the effects of air speed on condensation phenomena under different subcooling and airflow conditions. The analysis focuses on the following research questions:

(1) How does air speed affect the amount of condensation and the associated latent heat release?

(2) How does air speed influence the characteristics of the equivalent water thickness?

2 Method

To analyze the effects of elevated airflow on condensation phenomena on radiant cooling panels, a simplified numerical wind tunnel containing a cooling block (12 × 160 × 40 mm), representing a small-scale element of a commercial radiant cooling panel, was developed and CFD simulations were performed. The overall dimensions of the numerical wind tunnel are 240 × 240 × 1440 mm, and the geometry of the computational domain is shown in Figure 1.

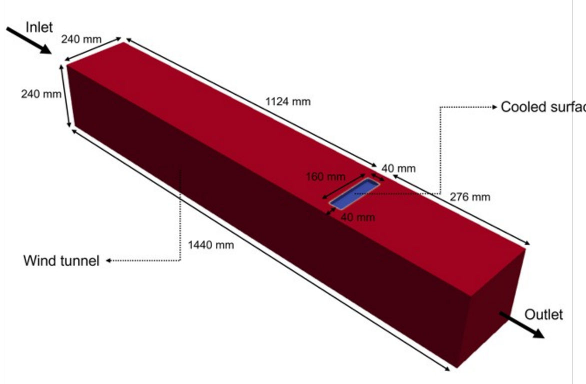

Figure 1. Simulation domain

The computational mesh was generated using snappyHexMesh [9], with locally refined grids applied near the radiant cooling panel surface to adequately resolve boundary-layer heat and mass transfer as well as water formation associated with condensation. After preliminary mesh convergence tests, the final mesh was determined to consist of 151,270 cells, with cell volumes ranging from 1.14×10^{-11} m³ to 2.56×10^{-6} m³. Mesh quality was verified using checkMesh, confirming that key quality metrics, including maximum non-orthogonality and skewness, were within acceptable ranges for the present simulations.

To accurately capture condensation behavior, the interThermalPhaseChangeFoam solver in OpenFOAM was employed [5]. This validated solver resolves mass transfer between gas and liquid phases and accounts for latent heat effects through coupling with the energy equation. All simulations were performed as transient simulations to capture the time-evolving nature of condensation.

Although condensation is inherently transient, this study focuses on the quasi-steady regime that is representative of sustained panel operation. The initial transient period is dominated by start-up effects and does not reflect the long-term balance between water generation and removal. After a short transient, key quantities converge and fluctuate within a narrow range. Preliminary simulations indicated that the equivalent water thickness reached a quasi-steady state within a few seconds of the simulation start. Therefore, a total simulation time of 10 s was applied for all cases.

To represent indoor conditions relevant to built environments, the inlet air temperature was prescribed in the range of 22.2-26.7 °C (72-80 °F), and the relative humidity was set to 50, 55, 60% [2]. To investigate condensation risk scenarios that may arise when accidental warm and humid outdoor air is introduced and mixed into indoor spaces via infiltration or an open window, the surface temperature of the radiant cooling panel was set to 0.5 °C, 1.0 °C, and 2.0 °C below the dew-point temperature of the inlet air. Air velocity was varied from 0 to 3 m/s to span indoor airflow conditions representative of fan-assisted spaces. According to example configurations in the CBE Fan Tool, fan operation can produce minimum local air speeds on the order of 0.5 m/s, with average air speeds commonly ranging from approximately 0.9 to 2.7 m/s depending on fan type and layout [10]. Based on the resulting Reynolds number range, RANS-based k–ω SST (kOmegaSST) turbulence model [6,8] was employed for the simulation.

Although the surface temperature of radiant cooling panels in actual buildings depends on chilled-water supply conditions, flow rates, and heat exchange with the surrounding environment, the panel was modeled using an idealized isothermal boundary condition in this study. This assumption was intentionally adopted to isolate the effects of airflow on condensation behavior by excluding confounding influences from spatially varying panel temperatures and temporal variations in hydronic operating conditions. All remaining walls were treated as adiabatic, and the outlet boundary was modeled as a pressure outlet.

At each timestep, the solver solves the following energy conservation equation:

$$\partial(\rho H)/\partial t + \nabla\cdot(\rho U H) = \nabla\cdot(k_{eff}\nabla T) - Q_{pc} \qquad (1)$$

where ρ is density, t is time, H is specific enthalpy, U is velocity vector, k_{eff} is effective thermal conductivity, T is temperature, and Q_{pc} is phase change heat source term. The left-hand side represents enthalpy accumulation and convective transport, and the right-hand side represents heat transfer by conduction, and phase change. Here, $k_{eff} = k + \rho C_p \nu_t$, where k is molecular thermal conductivity, Cp is specific heat capacity at constant pressure, and ν_t is turbulent kinematic viscosity.

Phase change at the liquid-vapor interface was modeled using the InterfaceEquilibrium model [5]. This model enforces thermal equilibrium at interface cells by applying a corrective energy source term such that the interface temperature is restored to the dew-point temperature at each time step. The phase change heat source term, Q_{pc}, is evaluated at interface cells as

$$Q_{pc} = \rho\cdot C_p\cdot(T_{cell} - T_{dewpt})/\,\Delta t \qquad (2)$$

Where ρ is the density, T_{cell} is the interface cell temperature, T_{dewpt} is the dewpoint temperature, and Δt is time step. $Q_{pc} < 0$ indicates condensation (latent heat release), while $Q_{pc} > 0$ denotes evaporation (latent heat absorption).

Q_{pc} is a modelled term strictly derived from the interfacial equilibrium assumption. Numerically, this term functions as the energy source required to offset the net sensible heat imbalance to satisfy thermal equilibrium at the interface. Bearing this in mind, we interpret Q_{pc} as the phase change heat that quantifies the latent heat release or absorption required to satisfy the equilibrium constraint at each time step [7].

For the conditions in this study, the surface temperature (T_{srf}), T_{dewpt}, and wind tunnel inlet air temperature (T_a) satisfy: $T_{srf} < T_{dewpt} < T_a$. Equations (1) and (2) are solved iteratively at each time step until the computed fields, including velocity, pressure, and enthalpy, converge to within six decimal places.

3 Results

3.1 Effect of airflow velocity and subcooling on phase change heat

Figure 2 presents the steady-state phase change heat flux per unit area over the panel as a function of air velocity under three subcooling conditions (ΔT = 0.5, 1.0, and 2.0 °C).

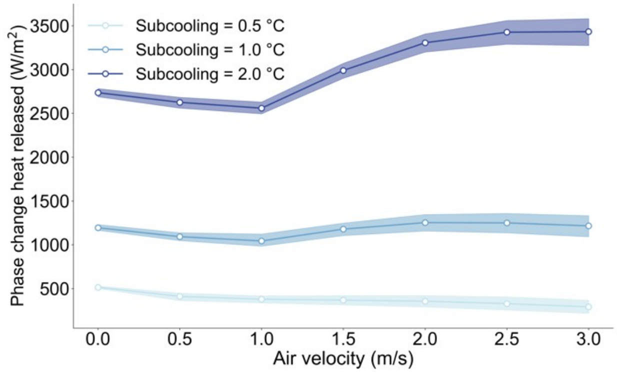

Figure 2. Relationship between air velocity and phase change heat released during steady state

Across all cases, the system reached a steady state rapidly, with the phase change heat entering and remaining within ±5% of the final mean value within an average of 0.7 s and a maximum of 2.1 s. The plotted values represent the mean phase change heat flux computed over the steady-state period following this convergence.

Here, the phase change heat release is obtained by integrating the phase-change heat source term (Q_{pc}) over the condensation region and normalizing by the panel area. Since the computed Q_{pc} values remain negative throughout the simulations, they indicate heat release due to condensation under the adopted sign convention. This reflects the integrated phase change behavior, in which condensation consistently dominates evaporation at each timestep. Therefore, the results are reported as the phase-change heat release, defined as the absolute value of the integrated Q_{pc}.

The magnitude of phase change heat depends on the competition between cooling and heating effects at the interface. Cooling is dominated by conductive heat transfer towards the cold surface, while heating arises primarily from convective heat transfer from the warm air. When convective heating exceeds conductive cooling, the interface temperature approaches the dew point, suppressing condensation. Conversely, dominant conductive cooling maintains the interface temperature further below the dew point, enhancing condensation.

3.1.1 Effect of subcooling on phase change heat

Under constant airflow conditions, phase change heat increased with increases in the level of subcooling. This trend results from enhanced conduction cooling at lower surface temperatures (high subcooling), which maintains the interface temperature further below the dew point.

3.1.2 Effect of air velocity on phase change heat

For the low subcooling condition (subcooling of 0.5°C) as shown in Figure 2, phase change heat decreased with increasing air velocity. At low subcooling, the temperature difference between the cooled surface and interface is small, resulting in weak conduction cooling. Although increasing airflow enhances the effective thermal conductivity through enhanced turbulent mixing and thereby strengthens surface conduction cooling, the convective heating from the warm air increases at a greater rate. Consequently, the interface temperature (T_{cell}) moves towards the dew point temperature (T_{dewpt}), leading to a reduction in phase change heat as air velocity increases.

In contrast, different trends were observed at higher subcooling conditions (subcooling of 1.0 °C and 2.0 °C). For both cases, the phase change heat initially decreased as air velocity increased from 0 to 1 m/s, which can be attributed to the same mechanism observed under low subcooling conditions. However, beyond 1 m/s, phase change heat has non-monotonic behavior. Specifically, at a subcooling of 2.0 °C, the phase change heat increased continuously over the velocity range of 1-3 m/s, although the rate of increase gradually diminished. At subcooling of 1.0 °C, the phase change heat increased over the range of 1-2 m/s with progressively decreasing slope, followed by a slight decrease in the 2-3 m/s range.

This non-monotonic behavior at higher subcooling can be explained by the competing effects of cooling and heating mechanisms at the interface. At high subcooling, conduction cooling from the cold surface is strong, and this cooling effect is further enhanced as increasing air velocity intensifies k_{eff} due to enhanced turbulent mixing. While convective heating from the warm air also increases with air velocity, when subcooling is sufficiently high, the enhanced surface conduction cooling outweighs convective heating. As a result, higher air velocities maintain the interface temperature at lower values despite increased convective heating, leading to increased phase change heat.

At sufficiently high air velocities, however, this trend weakens or reverses. Convective heating of the interface becomes increasingly dominant, causing the interface temperature to rise. As a result, the phase change heat either increases more slowly (at a subcooling of 2.0 °C) or slightly decreases (at a subcooling of 1.0 °C). This transition reflects a shift in the balance between conduction cooling and convective heating mechanisms.

3.2 Effect of airflow velocity and subcooling on equivalent water thickness

Figure 3 shows the equivalent water thickness obtained by normalizing the total liquid water volume remaining after 10 s of development by the cooled panel surface area. The results are grouped by subcooling condition using color coding, with air velocity shown on the x-axis and equivalent water thickness on the y-axis.

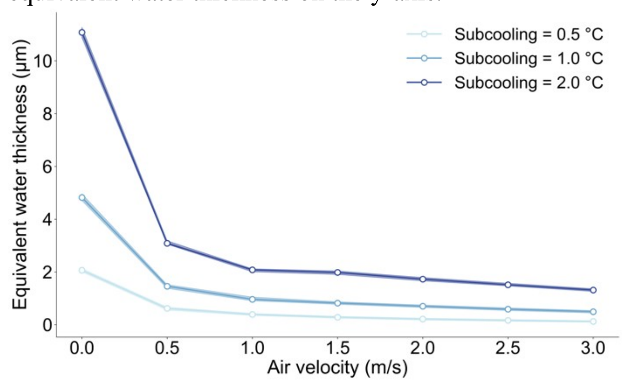

Figure 3. Relationship between air velocity and equivalent water thickness

First, the equivalent water thickness increases with increasing subcooling, which can be attributed to enhanced condensation under larger temperature differences between the cooled surface and the interface.

In contrast, for a given subcooling condition, the equivalent water thickness decreases with increasing air velocity. The liquid water formed on the surface is governed by a balance between condensation-driven accumulation and flow-induced removal. As air velocity increases, the boundary layer near the surface becomes thinner, resulting in steeper velocity gradients and increased wall shear stress. The increased shear promotes the transport and removal of liquid water along the surface, reducing the residence time of condensed water near the panel. Consequently, although condensation may still occur, the accumulated water becomes thinner at higher air velocities due to more efficient removal by the airflow.

As airflow increases, the equivalent water thickness decreases and the phase-change region shifts closer to the panel surface. This results in a steeper temperature gradient across the remaining interface and enhanced conduction cooling. This effect provides an additional contribution to the enhancement of conduction cooling with increasing airflow at high subcooling, alongside the increase in k_{eff} discussed in Section 3.1.2.

From a practical perspective, these results indicate that introducing even modest airflow may help mitigate liquid water accumulation on radiant panels during periods of condensation. Compared to stagnant air, airflow enhances the removal of condensed water from the surface, which may reduce the likelihood of droplet growth and dripping from the ceiling.

4 Conclusion

Radiant cooling panels have traditionally been controlled at water supply temperatures above the dew point to avoid the risk of condensation. However, this conservative operation has been reported to limit their cooling capacity. In this study, CFD simulations were conducted to investigate the effects of airflow on condensation phenomena when a uniformly cooled radiant panel operates below the dew point. Under identical airflow conditions, increasing subcooling resulted in increases in both phase change heat and equivalent water thickness. Second, the influence of airflow on phase change heat depended strongly on the subcooling level. At a low subcooling of 0.5 °C, increasing air velocity consistently suppressed condensation, whereas at higher subcooling levels (1.0 °C and 2.0 °C), phase change heat decreased at low air velocities (0-1.0 m/s) but increased at higher velocities, with diminishing or slightly reversing trends at the highest velocities. Third, the equivalent water thickness decreased with increasing air velocity across all subcooling conditions.

These results indicate that, in addition to enhanced convective heat transfer reported in previous studies [1], higher air velocities promote efficient removal of condensed water from the panel surface. Specifically, airflow velocities above 0.5 m/s consistently reduced equivalent water thickness across all subcooled conditions (ΔT = 0.5–2.0 °C), thereby reducing dripping risk. At velocities of 1.0 m/s and above, increasing airflow simultaneously enhanced latent heat removal through condensation while maintaining low water accumulation on the surface.

From an operational standpoint, these results suggest that during transient events involving the sudden inflow of warm and humid air, such as window opening or infiltration, increasing airflow can be an effective immediate response. In radiant cooling systems, adjustments to the cooling setpoint inherently involve time delays, and during this period elevated airflow can mitigate condensation-related issues such as dripping while simultaneously contributing to more rapid conditioning of the incoming humid air through enhanced latent heat removal.

These results demonstrate that when subcooling occurs, the associated condensation risks can be mitigated through appropriate airflow management. This understanding provides a foundation for developing control strategies that leverage airflow as an active parameter, offering operational flexibility beyond the conventional practice of strict dew point avoidance and enabling safer exploitation of the additional cooling capacity available under subcooled conditions.

Moreover, this study demonstrates that condensation risk cannot be adequately assessed using a single metric such as phase change heat or total condensed water alone. Instead, water removal and accumulation characteristics should be jointly considered when evaluating condensation risk under realistic operating conditions.

Finally, it should be noted that the present study is based on idealized CFD simulations that differ from real operating conditions of radiant cooling panels. In practice, the surface temperature of radiant cooling panels exhibits both spatial and temporal variations, and increased airflow may further modify the surface thermal conditions, leading to transient effects on condensation behavior. Future studies should extend these findings by considering transient surface temperature control, complex airflow patterns, and realistic spatial scales through experiments or high-resolution simulations.

References

Journal articles

1. C. Karmann, F. Bauman, P. Raftery, S. Schiavon, M. Koupriyanov, Effect of acoustical clouds coverage and air movement on radiant chilled ceiling cooling capacity, Energy Build. **158** (2018) 939–949. https://doi.org/10.1016/j.enbuild.2017.10.046.
2. J. Li, J. Pantelic, C.B. Merchant, K.W. Chen, I. Izuhara, R. Yuki, F.M. Meggers, S. Schiavon, Comparison of the environmental, energy, and thermal comfort performance of air and radiant cooling systems in a zero-energy office building in Singapore, Energy Build. **318** (2024) 114487. https://doi.org/10.1016/j.enbuild.2024.114487.
3. W. Zhang, J. Pan, N. Li, A. Yongga, Q. Zhang, Investigation of supply air parameters of a new method to control the condensation risk in radiant cooling panels, J. Build. Eng. **61** (2022) 105288. https://doi.org/10.1016/j.jobe.2022.105288.

4. S.S. Salins, S.A. Siddiqui, S.V.K. Reddy, S. Kumar, Experimental investigation on the performance parameters of a helical coil dehumidifier test rig, Energy Sources Part Recovery Util. Environ. Eff. **43** (2021) 35–53. https://doi.org/10.1080/15567036.2020.1814455.
5. M. Nabil, A.S. Rattner, interThermalPhaseChangeFoam—A framework for two-phase flow simulations with thermally driven phase change, SoftwareX **5** (2016) 216–226. https://doi.org/10.1016/j.softx.2016.10.002.
6. F. Menter, M. Kuntz, R. Langtry, Ten Years of Industrial Experience with the SST Turbulence Model, **4** (2003) 625–632.
7. A.S. Rattner, S. Garimella, Simple Mechanistically Consistent Formulation for Volume-of-Fluid Based Computations of Condensing Flows, J. Heat Transf. **136** (2014). https://doi.org/10.1115/1.4026808.

Proceedings

8. F. Menter, T. Esch, Elements of Industrial Heat Transfer Prediction, 16th Brazilian Congress of Mechanical Engineering (COBEM), Uberlandia, Brazil, 2001

Webpage

9. OpenFOAM Foundation, snappyHexMesh meshing guide, OpenFOAM Documentation (2024). https://www.openfoam.com/documentation/guides/latest/doc/guide-meshing-snappyhexmesh.html (accessed September 8, 2025).
10. P. Raftery, CBE Fan Tool, Cent. Built Environ. Univ. Calif. Berkeley (2019). https://cbe.berkeley.edu/fan-tool (accessed September 6, 2025).